Abstract: 2041

CDK7 and CDK12 inhibition result in distinct transcriptional effects

Nisha Rajagopal, Sydney Alnemy, Anthony D'Ippolito, Jason Marineau, David Moebius, Elliot Cooper, Matthew Eaton, John Carulli, Claudio Chuaqui, Eric Olson, Shanhu Hu

Syros Pharmaceuticals, 35 CambridgePark Drive 4th floor, Cambridge MA 02140

Introduction

Transcriptional dysregulation and overexpression are key dependencies in cancer. Thus, the major RNA Pol2 modifying enzymes CDK7 and CDK12 have emerged as attractive cancer therapeutic targets. CDK7 phosphorylates the Ser5 residue on the C-terminal domain (CTD) of RNA Pol2 causing initiation of transcription while CDK12 phosphorylates the Ser2 CTD of RNA Pol2 triggering elongation. Additionally, CDK7 plays a role in cell cycle control which may indirectly affect transcription of genes. Recent studies have shown that CDK12 inhibition results in increased usage of intronic polyadenylation sites and a subsequent decrease in the expression of long genes. DNA damage repair genes, which are longer than the average gene, are particularly affected by the inhibition of CDK12.

While the transcriptional effects of inhibiting CDK7 and CDK12 have been explored in isolation, a direct comparison in an isogenic system has not yet been reported. Here, we generated OV90 analog-sensitive (AS) cell lines for CDK7 and CDK12, allowing us to directly contrast the transcriptional effects of CDK7 and CDK12 inhibition via RNA-seq. We then compared AS inhibition to compound inhibition with SY-1365 (CDK7 selective covalent inhibitor) , SY-5609 (highly CDK7 selective non-covalent inhibitor) and AZ2242 (CDK12 selective non-covalent inhibitor). This study demonstrates that CDK7 and CDK12 inhibition have distinct effects on the transcriptome arguing for unique therapeutic roles of clinical inhibitors.

Creation of OV90 CDK7 and CDK12 analog sensitive cell lines

CDK7 and CDK12 are made "analog-sensitive" (AS) by introducing mutations at gatekeeper positions within their ATP-binding pockets that do not affect their kinase function but allow binding of the non-hydrolyzable purine analog, 3MB-PP1. Since 3MB-PP1 cannot bind the ATP binding pockets of other kinases this results in selective inhibition of CDK7 or CDK12 [4].

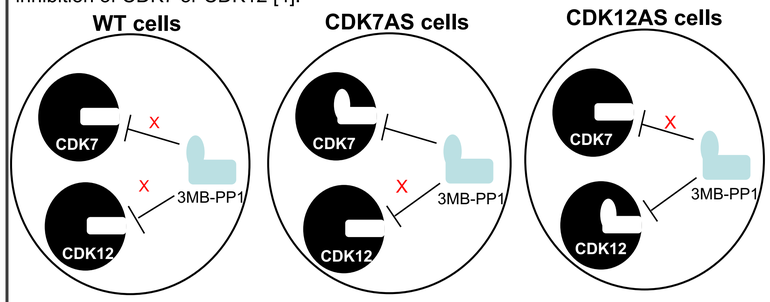

CDK7: Mutation F91G

CDK12: Mutation F813G + an AG→TG change to avoid erroneous splicing

Growth inhibition of cell lines upon inhibition of CDK7 and CDK12

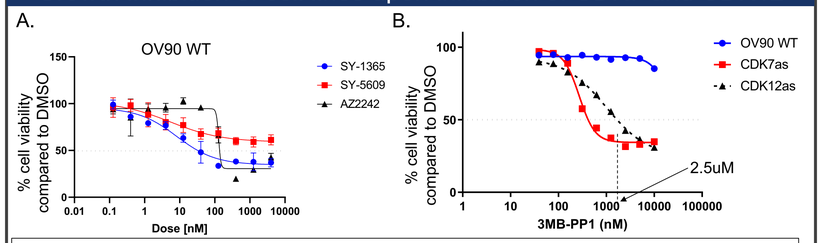

Growth inhibition of A.) OV90 WT cell line after 72hr of compound treatment, B) treatment of OV90 WT, CDK7As, and CDK12AS cell lines after 7 days of treatment with 3MB-PP1 as a percent of DMSO.

- 2.5uM of 3MB-PP1 was selected as the dose for RNA-seq as it resulted in at least 50% growth inhibition of the OV90 CDK7AS and CDK12AS cell lines.
- Low, medium and high doses for each compound were selected based on effects on anti-proliferation as well as other biochemical properties of the compound.

Transcriptional differences between CDK7AS and CDK12AS

- CDK7i and CDK12i share a significant overlap of down-regulated genes but also have distinct transcriptional effects.
- CDK7AS has more down-regulated genes but CDK12AS has the larger magnitude of downregulation upon 3MB-PP1 treatment.

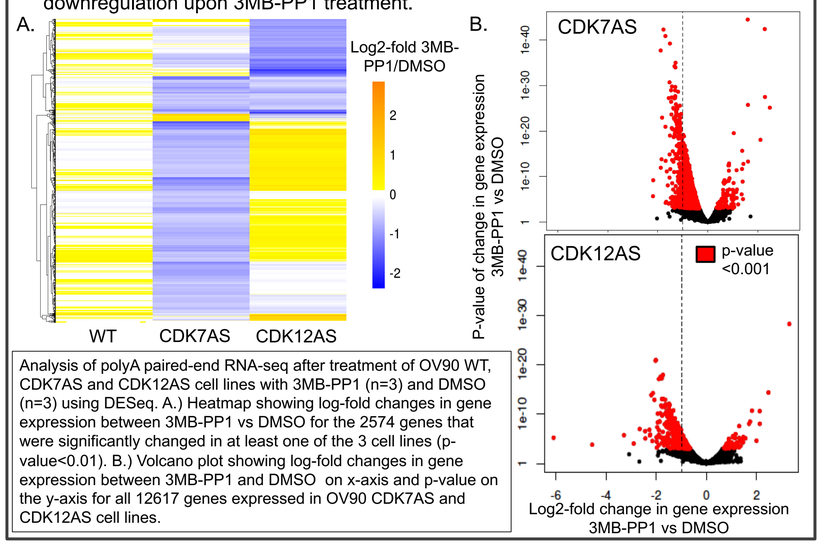

Analysis of polyA paired-end RNA-seq after treatment of OV90 WT, CDK7AS and CDK12AS cell lines with 3MB-PP1 (n=3) and DMSO (n=3) using DESeq. A.) Heatmap showing log-fold changes in gene expression between 3MB-PP1 vs DMSO for the 2574 genes that were significantly changed in at least one of the 3 cell lines (p-value<0.01). B.) Volcano plot showing log-fold changes in gene expression between 3MB-PP1 and DMSO on x-axis and p-value on the y-axis for all 12617 genes expressed in OV90 CDK7AS and CDK12AS cell lines.

Biochemical selectivity of compounds for CDKs is corroborated by concordance of gene expression changes in 3MB-PP1 treated AS cell lines and compound treatments

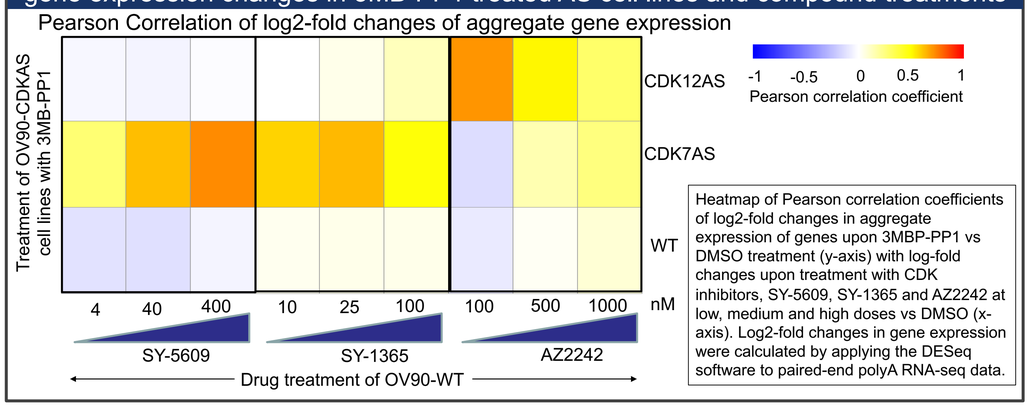

Heatmap of Pearson correlation coefficients of log2-fold changes in aggregate expression of genes upon 3MBP-PP1 vs DMSO treatment (y-axis) with log-fold changes upon treatment with CDK inhibitors, SY-5609, SY-1365 and AZ2242 at low, medium and high doses vs DMSO (x-axis). Log2-fold changes in gene expression were calculated by applying the DESeq software to paired-end polyA RNA-seq data.

Transcripts over 40kb long are significantly shortened by CDK12i but not CDK7i

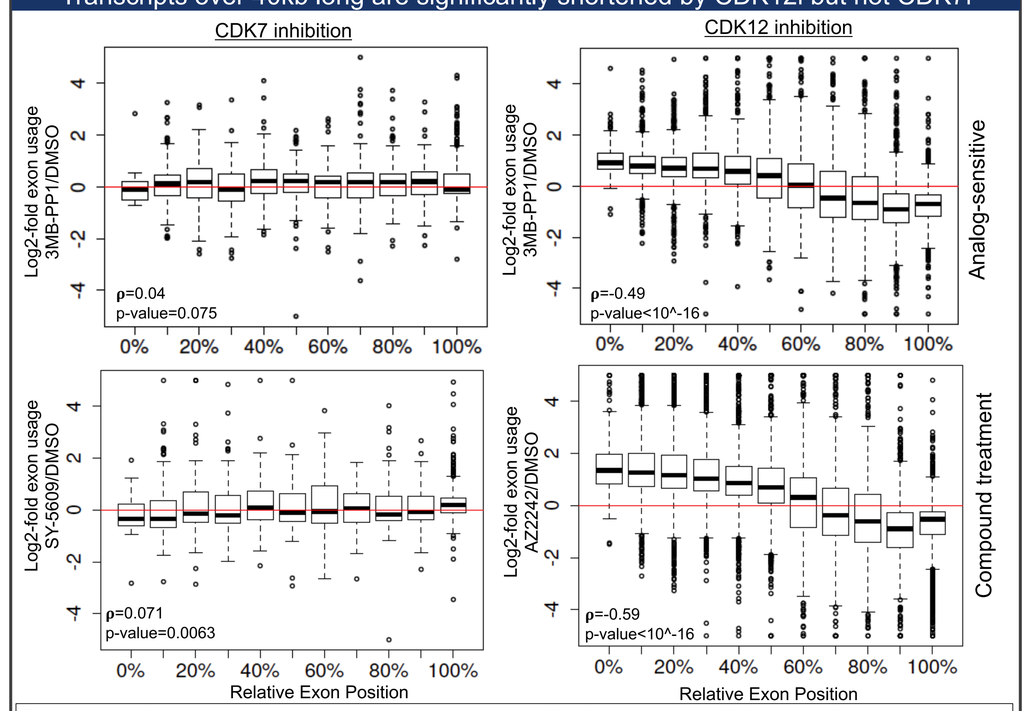

Exon usage significantly reduces with exon position along the gene upon CDK12 inhibition but not CDK7 inhibition. Relative exon position on the x-axis is defined as the grouping of exons into deciles based on their relative position along the gene. Exons with significant change in usage upon treatment (p-value<0.001) were identified by applying DEXSeq to RNA-seq data. Log2-fold change in exon usage compared to DMSO was then plotted against relative exon rank upon treatment of (clockwise, from top left to bottom right) OV90 CDK7AS with 3MB-PP1, OV90 CDK12AS with 3MB-PP1, OV90 WT with SY-5609 40nM, OV90 WT AZ2242 500nM.*

Genes over 40kb show significant transcript shortening in CDK12AS

AZ2242 shows shortening of the same transcripts observed to be shortened in CDK12AS

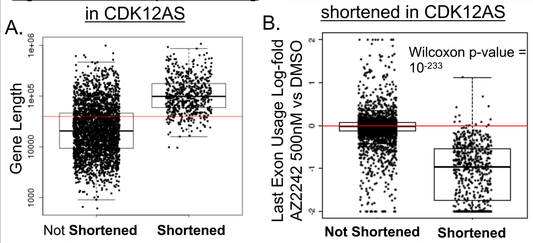

Transcripts grouped by shortening effect upon treatment of OV90 CDK12AS with 3MB-PP1

A. Transcripts significantly shortened in the OV90 CDK12AS cell line upon 3MB-PP1 treatment belonged to genes that were at least 40 kb long. Shortened transcripts were defined as those with significant reduction in exon usage upon 3MB-PP1 treatment from DEXSeq (p-value<0.001, log2-fold <-0.5) while unshortened transcripts were defined as those with a no reduction in last exon usage (log2-fold >=0). Shortened (n=575) and unshortened transcripts (n=2870) had maximum balanced accuracy of separation at 40kb at which threshold 90.3% of shortened transcripts were accurately predicted.*

B. Transcripts significantly shortened in the OV90 CDK12AS cell line upon 3MB-PP1 treatment showed significant reduction of last exon usage upon treatment with 500nM AZ2242 treatment compared to transcripts that were not shortened in the CDK12AS cell line. Shortened and unshortened transcripts are defined as above.*

* All boxplot statistics are as follows: box boundaries represent the inter-quartile range with the midline as the median of the data, whiskers extend to the most extreme data point that is less than or equal to 1.5 times the interquartile range from the boundary of the box.

Significantly shortened transcripts are enriched for DNA double-strand break repair

Shortened transcripts as well genes with downregulated expression upon CDK12 inhibition were enriched for the DNA double-strand repair pathway (Hypergeometric p-value < 0.01,GSEA p-value < 10^{-10} respectively)

Shortened transcripts defined as genes with significant decrease in last exon usage at p-value <0.01 as determined by DEXSeq

Exon usage along the exons of a key DNA damage repair gene, *RA54B*, shows significant reduction with exon position along the gene upon inhibition of CDK12 but not upon inhibition of CDK7. Exon usage was computed as proportion of reads assigned to each exon in the gene in any treatment. 3MB-PP1 and compound treatments are shown in red while DMSO is shown in black for reatment of (clockwise, from top left to bottom right) OV90 CDK7AS with 3MB-PP1 and DMSO, OV90 CDK12AS with 3MB-PP1 and DMSO, OV90 WT with SY-5609 40nM vs DMSO, OV90 WT AZ2242 500nM vs DMSO (figure to right)

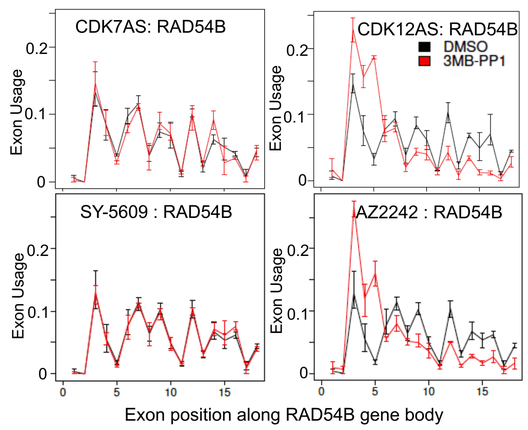

DNA damage observed upon CDK12 inhibition, but not CDK7 inhibition

gH2AX foci are increased upon AZ2242 treatment and high dose SY-1365 treatment while it is unchanged upon SY-5609 treatment suggesting DNA damage repair deficiency is induced by inhibition of CDK12 and not CDK7

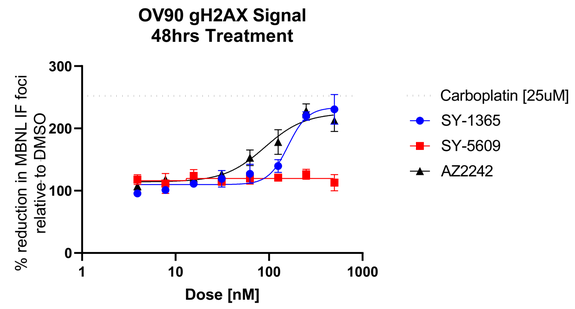

Relative change in mean gH2AX foci per nucleus upon treatment of OV90 WT cells with SY-1365, SY-5609 and AZ2242 at various concentrations for 48 hours compared to DMSO treatment. OV90 WT cells were fixed and stained with anti-gH2AX antibody to perform immunofluorescence microscopy. Each point represents the average number of gH2AX foci per nuclei normalized to % DMSO per plate across 3 experiments

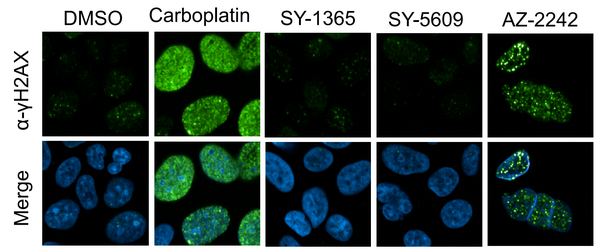

Representative image showing gH2AX foci change upon treatment of OV90 WT cell line with DMSO, Carboplatin at 25uM , and SY-1365, SY-5609 and AZ2242 at 125nM each (left to right). OV90 WT cells were fixed and stained with an anti-gH2AX antibody (green) and a Hoechst-33342 counterstain (blue). Images were acquired at 40X magnification using confocal microscopy on the Operetta CLS high-content microscope (Perkin Elmer).

Conclusions

- Inhibition of CDK7 and CDK12 result in distinct as well as shared transcriptional effects.
- Transcriptional effects induced by the compounds targeting CDK7 and CDK12 are highly concordant with the effects induced by selective manipulation of their target using an analog-sensitive system.
- Significant effects of CDK12 inhibition on transcript shortening observed that are not observed upon CDK7 inhibition.
  - supported by AS system as well as compound.
- Transcripts shortened by CDK12i are enriched for DNA double-strand break repair genes.
- Induction of DNA damage observed only upon inhibition of CDK12 but not CDK7 based on compound treatment.
  - Could be due to shortening of long DNA damage repair genes by CDK12i but not CDK7i.

References

1. S. Hu *et al.*, Discovery and Characterization of SY-1365, a Selective, Covalent Inhibitor of CDK7. *Cancer Res* **79**, 3479-3491 (2019).
2. S. Hu *et al.*, SY-5609, An orally available selective CDK7 inhibitor, demonstrates broad anti-tumor activity in vivo. *AACR Annual Meeting,*, Atlanta, Georgia, USA 2019.
3. L. Johannessen *et al.*, Pre-clinical evaluation of PK,PD and anti-tumor activity of the oral, non-covalent, potent and highly selective CDK7 inhibitor, SY-5609, provides rationale for clinical development in multiple solid tumor indications. *31st EORTC-NCI-AACR Symposium*, Boston, MA, 2019.
4. A. Koch, S. Hauf, Strategies for the identification of kinase substrates using analog-sensitive kinases. *Eur J Cell Biol* **89**, 184-193 (2010).
5. S. J. Dubbury, P. L. Boutz, P. A. Sharp, CDK12 regulates DNA repair genes by suppressing intronic polyadenylation. *Nature* **564**, 141-145 (2018).
6. A. P. Chirackal Manavalan *et al.*, CDK12 controls G1/S progression by regulating RNAPII processivity at core DNA replication genes. *EMBO Rep* **20**, e47592 (2019).
7. M. Krajewska *et al.*, CDK12 loss in cancer cells affects DNA damage response genes through premature cleavage and polyadenylation. *Nat Commun* **10**, 1757 (2019).
8. J. W. Johannes *et al.*, Structure Based Design of Selective Non-covalent CDK12 Inhibitors. *ChemMedChem* **13**, 231-235 (2018).

Cancer Epigenetics: New Mechanisms and Therapeutic Opportunities **Keystone Symposium**, Keystone, CO, USA **JAN 28, 2020**